

# A thermodynamic model for shear-induced concentration banding and macromolecular separation

D. Jou<sup>a,b,\*</sup>, M. Criado-Sancho<sup>c</sup>, L.F. del Castillo<sup>d</sup>, J. Casas-Vázquez<sup>a</sup>

<sup>a</sup>Departament de Física, Universitat Autònoma de Barcelona, 08193 Bellaterra, Catalonia, Spain

<sup>b</sup>Institut d'Estudis Catalans, Carme 47, 08001 Barcelona, Catalonia, Spain

<sup>c</sup>Departamento de Ciencias y Técnicas Físicoquímicas, UNED, Senda del Rey s/n, 28040 Madrid, Spain

<sup>d</sup>Instituto de Investigaciones en Materiales, UNAM, Apartado Postal 70-360, México DF 04510, Mexico

Received 24 July 2000; received in revised form 19 January 2001; accepted 22 January 2001

## Abstract

We present a simple thermodynamic model for shear-induced concentration banding in polymer solutions, based on a nonequilibrium chemical potential depending on the shear rate. This dependence provides a coupling between diffusion and shear, besides the more classical coupling provided by the divergence of the viscous pressure tensor. When both couplings are taken into account, shear-induced concentration banding appears in a natural way. If the initial homogeneous concentration is higher than a threshold value, shear banding appears for sufficiently high value of the shear rate  $\dot{\gamma}$ ; if the initial concentration is lower, the steady-state concentration profile under shear is smooth. The banding profile depends on the polymer molecular mass and therefore it provides a basis for the chromatographic separation of polymers of different molecular mass. © 2001 Elsevier Science Ltd. All rights reserved.

**Keywords:** Viscous pressure; Shear-induced concentration banding; Macromolecules

## 1. Introduction

Shear-induced phenomena in suspensions or solutions, as for instance migration and phase separation, are an active topic of research [1–3]. There is currently a live discussion about the relative importance of the thermodynamic and the dynamic contributions to these phenomena, i.e. whether they may be attributed to a non-equilibrium modification of the chemical potential or are due to a purely dynamical coupling between viscous pressure and diffusion. Here we will deal with this topic by starting from a generalised constitutive equation for the diffusion flux as applied to shear-induced concentration banding and its application to molecular separation.

A well-known constitutive equation for the solute diffusion flux  $J$  in the presence of viscous pressure is [4–8]

$$J = -\tilde{D}\nabla\mu_{\text{eq}} - \frac{D}{RT}\nabla\cdot P^{\text{v}} \quad (1)$$

with  $\mu_{\text{eq}}$  the local-equilibrium chemical potential of the solute,  $P^{\text{v}}$  the viscous pressure tensor,  $D$  the classical diffusion coefficient and  $\tilde{D}$  a transport coefficient related to  $D$

through the relation  $D = \tilde{D}(\partial\mu_{\text{eq}}/\partial n)^{-1}$ , with  $n$  the solute concentration (in moles per unit volume). The viscous pressure tensor, also called by some authors as viscous stress tensor, is defined in terms of the total pressure tensor  $\mathbf{P}$  and of the equilibrium pressure  $p$  as  $\mathbf{P}^{\text{v}} = \mathbf{P} - p\mathbf{U}$ , with  $\mathbf{U}$  the unit tensor. The second term in this equation describes a coupling between viscous pressure and diffusion. Its physical interpretation is rather clear: minus the divergence of the viscous pressure tensor contributed by the polymer is the local net force density on the polymer chains and these respond by moving in the direction of this force.

In several papers [3,9–13] we have explored the consequences of a generalisation of Eq. (1), where instead of the local-equilibrium chemical potential, a generalised chemical potential depending on the viscous pressure is used. This chemical potential arises in a natural way in thermodynamic theories as extended irreversible thermodynamics (EIT) [14–18], where the thermodynamic functions depend on the dissipative fluxes acting on the system, or in theories with internal variables [19–20], where the microstructural details of the system (as for instance the molecular configuration tensor) are taken into account. In this way, a double coupling of diffusion with viscous pressure appears in Eq. (1): a linear dependence on the divergence of  $\mathbf{P}^{\text{v}}$  given by the second term, and a quadratic dependence on  $\mathbf{P}^{\text{v}}$

\* Corresponding author. Tel.: +34-93-5811563; fax: +34-93-5812155.  
E-mail address: jou@circe.uab.es (D. Jou).

through the generalised chemical potential in the first term. Indeed, in equilibrium thermodynamics it is well known that chemical potential gradients are different from concentration gradients, and may have different sign in some occasions. The new aspect of our work is to include non-equilibrium effects due to the flow in the chemical potential. These effects are not present, of course, in equilibrium theories, but turn out to play a relevant role in the dynamics of polymer separation, as it has been shown in [12] in connection with the experimental results reported in [22].

By using for the chemical potential the expression derived from EIT [14–18] we have evaluated the contributions of both terms to the shear-induced shift of the spinodal line of polymer solutions under flow [3,9–11] and shear-induced polymer migration [12,13]. The purpose of this paper is to apply this analysis to shear-induced concentration banding, namely, the appearance of bands of different concentrations under the action of a viscous pressure in an initially homogeneous polymer solution [21,22].

This phenomenon may have practical outcomes in new methods of chromatography, i.e. for separation of macromolecules of different mass [1,23–25], as in other technical and biological situations, because the banding profile depends on the molecular mass. Note that in the literature the expression shear banding may also refer to a different situation [26–30] in which bands of different shear rate, rather than of different concentrations, appear, but here we focus our attention on concentration effects. In Section 2 we give the expression of the generalized chemical potential incorporating the effect of the flow. In Section 3 we use it to describe concentration banding and in Section 4 we apply it to analyze molecular separation after having considered the mass dependence of the concentration profile derived in the Section 3.

## 2. Chemical potential under flow

To describe the evolution of concentration, the constitutive equation (1) must be complemented with an equation of state for the chemical potential. In EIT [13–16], the chemical potential depends not only on temperature, pressure and concentration but also on the viscous pressure and it is given by [3,12]

$$\mu(T, p, c, \mathbf{P}^v) = \mu_{\text{eq}}(T, p, c) + \frac{1 - \bar{V}_n}{4V} \frac{\partial(JV)}{\partial n} \mathbf{P}^v : \mathbf{P}^v, \quad (2)$$

where  $V$  is the volume of the system,  $\bar{V} = (\partial V / \partial n)_{T, p, n_0, \mathbf{P}^v}$  the partial molar volume of the solute, and  $J$  the so-called steady-state compliance defined as  $J = \tau / \eta$  (with  $\tau$  effective relaxation time and  $\eta$  the total viscosity of the solution) from a qualitative perspective, the contribution depending on  $\mathbf{P}^v$  describes the stored elastic free energy in the chains stretched by the flow.

Introduction in Eq. (1) of the generalised chemical potential (2) instead of the local-equilibrium chemical potential

yields

$$J = -D_{\text{eff}} \nabla c - \frac{D}{RT} \nabla \cdot \mathbf{P}^v, \quad (3)$$

where  $D_{\text{eff}}$  is an effective diffusion coefficient defined by [12]

$$D_{\text{eff}} = \frac{D}{(\partial \mu_{\text{eq}} / \partial n)} \left( \frac{\partial \mu}{\partial n} \right) = D \left\{ 1 + \frac{1}{(\partial \mu_{\text{eq}} / \partial n)} \frac{\partial}{\partial n} \left[ \frac{1 - \bar{V}_c}{4V} \frac{\partial}{\partial n} (JV) \mathbf{P}^v : \mathbf{P}^v \right] \right\} \quad (4)$$

As it is seen in Eq. (4),  $D_{\text{eff}}$  depends explicitly on the viscous pressure.

In Fig. 1 we plot the effective diffusion coefficient  $D_{\text{eff}}$  calculated according to expression (4) as a function of the reduced concentration  $\tilde{c} (= [\eta]nM)$ , with  $M$  the solute molecular mass and  $[\eta]$  the intrinsic viscosity, for a solution of high molecular mass polystyrene ( $M = 2000 \text{ kg/mol}$ ) in oligomeric polystyrene of  $0.5 \text{ kg/mol}$ , at  $0.20 \text{ wt\%}$  (the system so called 2 M in Ref. [22]) for different values of the shear rate. To obtain it, we used for the viscous pressure tensor an upper-convected Maxwell model together with a Rouse–Zimm model for the steady-state compliance and the viscosity [9], and we considered a cone–plate device, where the only nonvanishing components of the viscous pressure are [22]

$$\mathbf{P}_{\phi\phi}^v = 2RTn(\tau\dot{\gamma})^2; \quad \mathbf{P}_{\theta\theta}^v = RTn\tau\dot{\gamma}, \quad (5)$$

where  $\phi$  and  $\theta$  refer to the axial and azimuthal directions, respectively, in such a way that the double contraction of  $\mathbf{P}^v$  is given by

$$\mathbf{P}^v : \mathbf{P}^v = 2(nRT)^2 [2(\tau\dot{\gamma})^4 + ((\tau\dot{\gamma})^2)]. \quad (6)$$

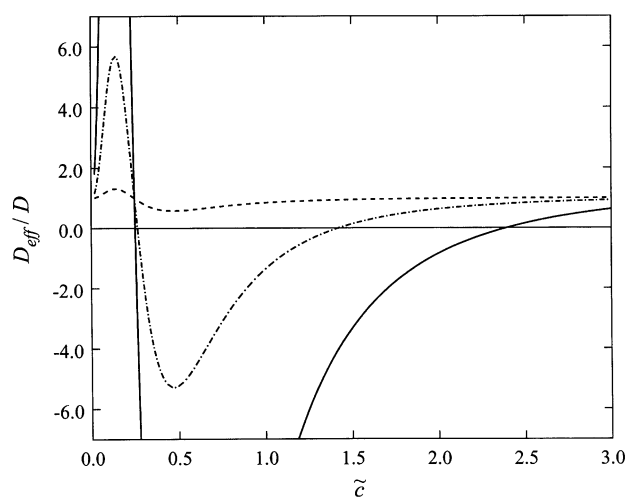


Fig. 1. Ratio  $D_{\text{eff}}/D$  calculated from Eq. (4) as a function of the concentration for three values of the shear rate (continuous curve  $1.5 \text{ s}^{-1}$ , dashed and dot curve  $1.0 \text{ s}^{-1}$  and dashed curve  $0.5 \text{ s}^{-1}$ ). The system considered is polystyrene with a molecular mass  $2000 \text{ kg mol}^{-1}$  solved in oligomeric polystyrene [22].

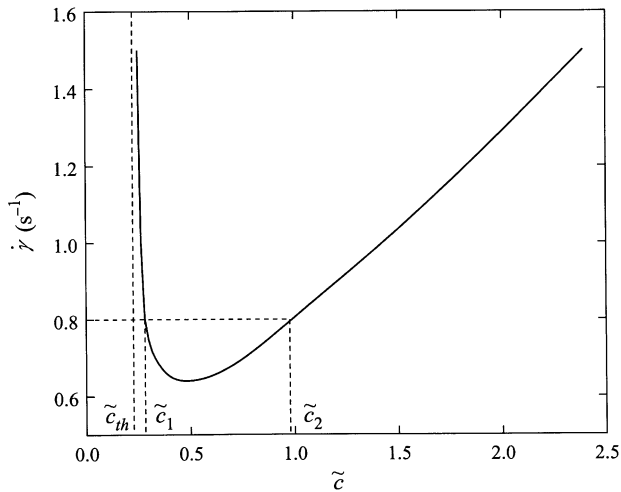


Fig. 2. For values of shear rate and concentration in the region above the curve in this Figure, the effective diffusion coefficient  $D_{\text{eff}}$  is negative and therefore the initially homogeneous system splits in two regions with different concentrations. For a given value of  $\dot{\gamma}$ , the values of the concentration near the apex and near the edge are given by the intersection of the horizontal line corresponding to the value of  $\dot{\gamma}$  with the curve plotted in the Figure. The minimum of this curve corresponds to the threshold value of  $\dot{\gamma}$  for shear banding.

It is seen in Fig. 1 that for  $\dot{\gamma}$  higher than a threshold value,  $D_{\text{eff}}$  is negative for concentration values between  $\tilde{c}_1$  and  $\tilde{c}_2$ , which depend on  $\dot{\gamma}$  (especially the upper value  $\tilde{c}_2$ , whereas the lower one is relatively insensitive to  $\dot{\gamma}$ ). The negative contribution to  $D_{\text{eff}}$  may be interpreted by saying that the stored elastic free energy per chain is higher in a region of large compliance (at constant stress). Accordingly, at fixed stress chains will migrate away from regions of low concentration, where compliance is higher. For some values of  $\tilde{c}$  and  $\dot{\gamma}$ , this tendency may overcome the usual tendency to flow from higher to lower concentration, which is described by the first term in Eq. (4).

Fig. 2 shows the domain of values of  $\tilde{c}$  and  $\dot{\gamma}$  for which  $D_{\text{eff}}$  is negative (at given  $T$  and  $p$ ): this corresponds to the region above the curve, which has a minimum for a given critical value  $\dot{\gamma}_c$  of the shear rate. In fact, this curve is nothing but the spinodal line in the  $\tilde{c} - \dot{\gamma}$  plane, as it corresponds to the limit of stability of the solution. For a fixed  $\dot{\gamma}$ , the values of  $\tilde{c}_1$  and  $\tilde{c}_2$  are given by the intersection of this curve with the corresponding horizontal line. Note the threshold  $\tilde{c}_{\text{th}}$ , below which the effective diffusion coefficient is always positive: banding would not be present for concentrations lower than this value.

### 3. Shear-induced concentration banding

Figs. 1 and 2 suggest directly a mechanism for shear banding. Assume one starts from an homogeneous solution with initial concentration  $\tilde{c}_0$  and that one imposes on the system a constant shear rate by rotating the cone at suitable angular speed. The second term in Eq. (1) always produces a

flux of solute towards the apex of the cone [12,21]. When  $D_{\text{eff}}$  is positive, this flux will be opposed by the concentration-driven diffusion flux and an (usually smooth) inhomogeneous steady state will be reached eventually. If, in contrast,  $D_{\text{eff}}$  is negative, the inhomogeneization process will be much faster because the flux produced by  $\nabla \cdot \mathbf{P}^v$  will be amplified. This gives separation times two orders of magnitude lower than those predicted when  $D_{\text{eff}}$  is positive [12], in agreement with the experimental results in [22].

This fast migration will eventually lead to a steady state in which the system will be split in two different bands, as sketched in Fig. 3. The inner band will have a high solute concentration approximately equal to  $\tilde{c}_2$  and the outer one a low solute concentration approximately equal to  $\tilde{c}_1$  separated by a rather sharp region with a steep concentration gradient. The conditions imposed on the profile are  $\tilde{c} = \tilde{c}_1$  for  $x = 1$  and  $\tilde{c} = \tilde{c}_2$  for  $x = 0$ , with  $x = r/R$ ,  $r$  being the distance to the apex and  $R$  the outer radius of the device. In fact, this profile will be rounded-off as a compromise between the migration towards the centre due to the second term in Eq. (3) and the outgoing diffusion driven by the concentration gradient in the regions with positive  $D_{\text{eff}}$  but the detailed numerical analysis is far from trivial; furthermore, our purpose here is not the obtention of the explicit form of the profile, but rather to illustrate a criterion for the conditions under which shear-induced concentration banding is expected to occur.

For initial inhomogeneous concentration higher than  $\tilde{c}_{\text{th}}$  (the lowest concentration for which  $D_{\text{eff}}$  may become negative for sufficiently high  $\dot{\gamma}$ , according to Fig. 2) banding will appear for values of the shear rate higher than the ones

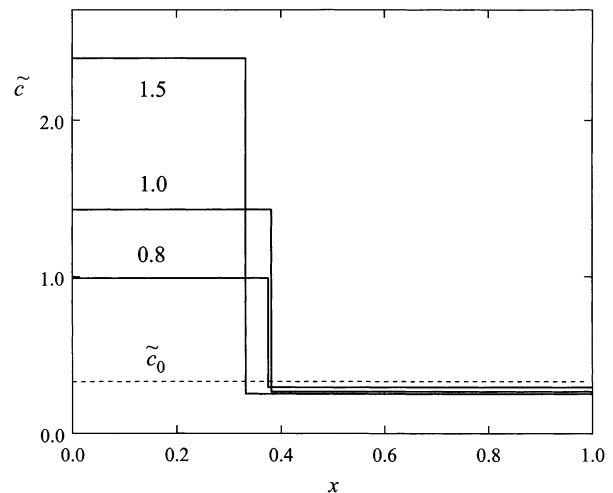


Fig. 3. Sketch of the steady-state concentration profile in a cone-and-plate device for three different values of the shear rate ( $1.5 \text{ s}^{-1}$ ,  $1.0 \text{ s}^{-1}$  and  $0.8 \text{ s}^{-1}$ ) as a function of the ratio  $x = r/R$  of the distance  $r$  to the apex of the cone and the outer radius  $R$  of the device. The initial homogeneous concentration value  $\tilde{c}_0$  is higher than the critical value  $\tilde{c}_c$ . The region of steep increase is determined by mass conservation in the device, and the inner and outer concentrations correspond to  $\tilde{c}_2$  and  $\tilde{c}_1$ , respectively. In actual situations, the profile will be rounded off due to the influence of the last term in Eq. (3).

corresponding to Fig. 2. Goveas and Fredrickson [21] have obtained a similar behaviour in their theoretical analysis of banding in a polymer solution in a wide-gap Couette flow between two coaxial cylinders; a steep part in the concentration profile appears for sufficiently high values of the shear rate. They use for the chemical potential the local-equilibrium form and the concentration inhomogeneity is due in their model only to the term  $\nabla \cdot \mathbf{P}^v$  in Eq. (3). The nonequilibrium chemical potential used in our work amplifies the separation rate and the steepness of the profile. The support of this evidence was given by the comparison of our result with the experimental data obtained by MacDonald and Muller [13,22].

Nozières and Quemada [26], in an analysis of the hydrodynamic stability of suspensions flowing along a cylindrical tube, have also found under some circumstances a negative diffusion coefficient, which is seen to be related to unstable fluctuations which break the system in different bands or domains. Let us finally stress that this analysis does not exclude the possibility of other influences on shear banding. For instance, some models [6] assume a strong dependence of the rheological coefficients (viscosity, normal stress coefficients) on the concentration, which in this way couple to diffusion and contribute to induce migration. The fact that in our model this dependence is not necessary for banding does not preclude that it may exist and further enhance the effects considered here.

#### 4. Shear-induced chromatography

Chromatographic techniques, i.e. the separation of different molecules initially mixed, have obvious and very wide applications [23–25]. Here, we study how the coupling between diffusion and flow considered in the Section 3 may provide a basis for macromolecular separation.

In Fig. 4 we plot the limit of the region where  $D_{\text{eff}}$  is negative in the plane of shear rate  $\dot{\gamma}$  versus reduced concentration  $\tilde{c}$  for three different molecular masses (2000, 3000 and 4000 kg/mol, respectively) of macromolecular polystyrene in oligomeric polystyrene. Fig. 4 generalizes Fig. 2, in which the region of negative  $D_{\text{eff}}$  was plotted only for a single molecular mass ( $M = 2000$  kg/mol). As in Fig. 2, for a given value of the concentration  $\tilde{c}$ ,  $D_{\text{eff}}$  becomes negative if the value of the shear rate is higher than the value indicated by the curve. According to the experimental data, the critical value  $\dot{\gamma}_c$  corresponding to the minimum of the curves is seen to depend on the macromolecular mass as  $\dot{\gamma}_c(M) \propto M^{-1.35}$ .

From this graph it is easy to find a semiquantitative description of the mass separation process. Of course, the detailed numerical analysis would be much cumbersome, but a simplified semiquantitative analysis is much useful in understanding the role of  $D_{\text{eff}}$  in the separation process.

Here, we will illustrate with two different situations the physical process. We consider a solution of three kinds of

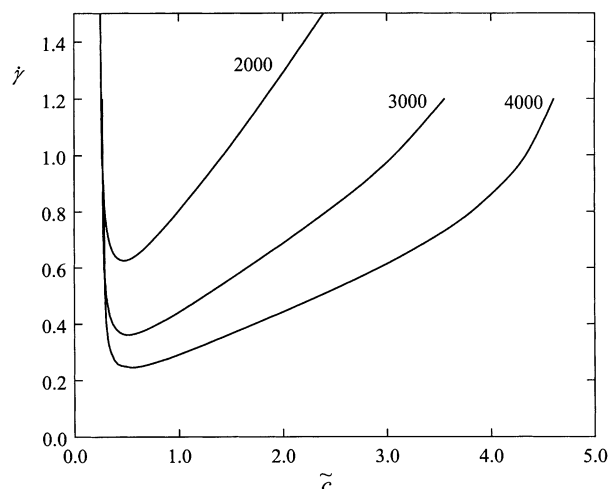


Fig. 4. For values of shear rate and concentration in the region above the curve in this Figure, the effective diffusion coefficient  $D_{\text{eff}}$  is negative, for solutions of macromolecular polystyrene with  $M = 2000, 3000$  and  $4000$  kg/mol, respectively, solved in oligomeric polystyrene of  $0.5$  kg/mol.

macromolecular polystyrene, of respective masses 2000, 3000 and  $4000 \text{ kg mol}^{-1}$  in oligomeric polystyrene. We assume, for the sake of simplicity, that the reduced concentration of these three species is initially the same, namely  $\tilde{c}_0 = 0.5$ , in an homogeneous solution in the cone-and-plate device considered in Section 3. As a further simplification, we assume that the concentration is low enough that the different macromolecular species behave independently of each other. Of course, these drastic simplifications may be removed at the price of more effort. We aim to describe the concentration profile of the three kinds of macromolecular species in the steady state reached after a sufficiently long time of rotation of the cone.

First, we consider a shear rate  $\dot{\gamma} = 0.35 \text{ s}^{-1}$ . The point corresponding to the initial conditions of the system is situated in the region where  $D_{\text{eff}}$  is negative for the macromolecules of  $M = 4000$ , but it is positive for the two other molecular species. Thus, the concentration of the latter ones will vary slightly on the position, with a slight tendency to accumulate near the apex. In contrast, since  $D_{\text{eff}}$  is negative for macromolecules of  $M = 4000$ , the system will split into two different regions: one near the centre, with a high concentration of  $M = 4000$  macromolecules, and another with a low concentration near the wall. The values of these two concentrations are given approximately by the intersection of the horizontal line corresponding to  $\dot{\gamma} = 0.35 \text{ s}^{-1}$  with the curve labelled 4000 in Fig. 4. This situation is depicted schematically in Fig. 5a, where the almost-vertical part of the profile has been calculated from the mass conservation condition. As it is seen in Fig. 2, the central zone will be rich in molecules with  $M = 4000$ .

The second situation corresponds to a shear rate  $\dot{\gamma} = 1.0$ . For this value of  $\dot{\gamma}$  and for  $\tilde{c}_0 = 0.4$ ,  $D_{\text{eff}}$  is negative for the three macromolecular species. Now, the system will split

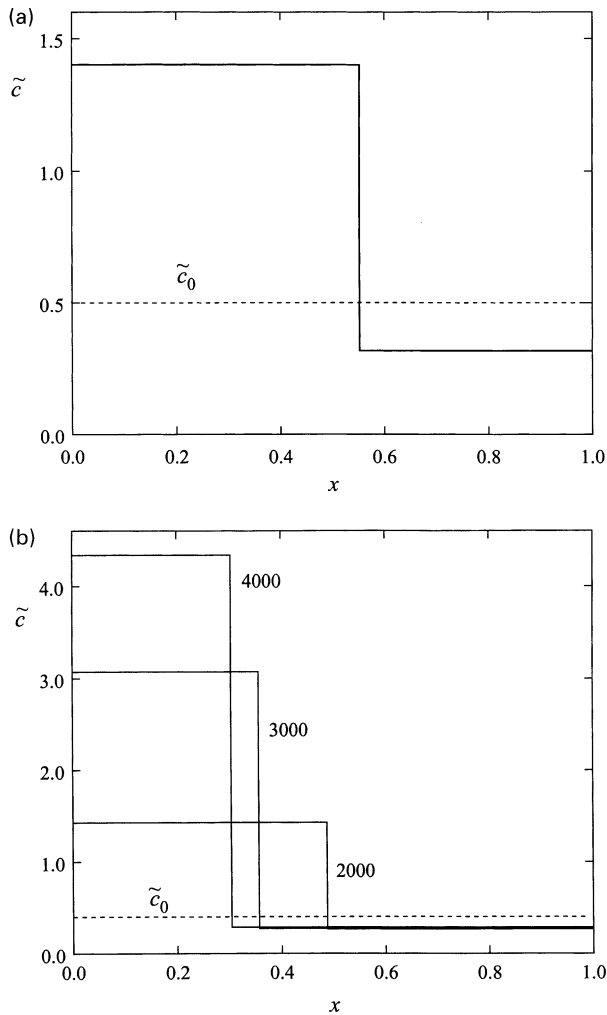


Fig. 5. Concentration profiles of polystyrene macromolecules of different molecular mass under shear viscous pressure. Fig. 5a and b correspond to different initial homogeneous conditions, detailed in the text.

into two regions for each species: a central one, rich in the species, and an external one, with a low concentration. The values of the concentration near the central region and in the external region are given approximately by the intersection of the horizontal line corresponding to  $\dot{\gamma} = 1 \text{ s}^{-1}$  with the three corresponding curves plotted in Fig. 4. The situation is depicted in Fig. 5b when the same initial concentration  $\tilde{c} = 0.4$  is supposed for all the species.

A third possibility could be, for instance, that  $\dot{\gamma} = 1 \text{ s}^{-1}$  but that the initial reduced concentration of  $M_2$  is 1.0 (it is inside the zone with  $D_{\text{eff}}$  negative) whereas  $\tilde{c} = 2.0$  for  $M_3$  and  $M_4$  macromolecules (thus corresponding to positive  $D_{\text{eff}}$ ). In this case, the concentration of  $M_3$  and  $M_4$  in the steady state will depend only slightly on the position whereas that of  $M_2$  near the apex will be enhanced with respect to its value in the initial homogeneous situation.

The actual values of the central and the external concentrations are not strictly equal to the value obtained in the mentioned intersections in Fig. 4, but must take into account the correction due to the

influence of the second term in Eq. (3). Anyway, this semi qualitative analysis of these two situations is, in our opinion, sufficiently illustrative of the fact that the nonequilibrium chemical potential predicts a separation process of the macromolecular species as a function of their mass. Note that the concentration band separation is more marked at lower Deborah numbers ( $\tau\dot{\gamma}$ ) for higher molecular weight: the same conclusion was reached in Ref. [21]. Of course, further analysis is necessary either to get higher precision as to apply it to other initial conditions. We hope that this short presentation may look sufficiently promising to encourage further development of this approach.

## 5. Concluding remarks

Shear-induced effects in polymer solutions are a very interesting field of research for nonequilibrium thermodynamics, because of the interplay between dynamical and thermodynamical effects. In this paper we have shown that the analysis of the effects of a generalized chemical potential including the nonequilibrium contributions of the viscous pressure, which has already been shown to drastically accelerate the shear-induced separation process [12,13,22], may be also useful to give a qualitative description of shear-induced concentration banding and of shear-induced macromolecular separation. Detailed quantitative analysis should solve in detail the dynamical equation (3) combined with the equation of state (2).

In fact, in this paper we have studied the limits of stability, i.e. the concentrations corresponding to the spinodal line rather than to the coexistence line. To obtain the latter, one should analyse in detail the relation between the chemical potential of the solute in both phases. In equilibrium, the equality of such chemical potential yields the equal-area Maxwell construction to determine the concentrations at the coexistence situation. However, when the divergence of the viscous pressure tensor in Eq. (3) does not vanish, the condition of vanishing diffusion flux would lead to different values for the chemical potential at different phases, as found from integration of Eq. (3). This could imply modifications of the Maxwell construction in non-equilibrium steady states. Since this topic is of special fundamental interest, it will be analysed in the future.

The concept of an effective diffusion coefficient to determine the limit of stability of the homogeneous solution has also been used by Milner [31] in a dynamical description of coupled concentration fluctuations and stress in an entangled polymer solution, based on a two-fluid model of the polymer and solvent dynamics. He studied a plane Couette flow along the  $x$  axis, with velocity profile given by  $v_x(y) = \dot{\gamma}y$  and obtained an anisotropic effective diffusion coefficient whose components along the  $y$  and  $z$  axis

were

$$D_{\text{eff}}(\hat{\mathbf{q}} = \hat{\mathbf{y}}) = D + \zeta^{-1}(\eta\dot{\gamma})^2 \left[ \frac{\alpha - 1}{2} \frac{\partial J}{\partial n} - \frac{\partial(\psi_y/\eta^2)}{\partial n} \right],$$

$$D_{\text{eff}}(\hat{\mathbf{q}} = \hat{\mathbf{z}}) = D + \zeta^{-1}(\dot{\gamma})^2 \left[ \frac{\alpha - 1}{2} \frac{\partial(J\eta^2)}{\partial n} - \frac{\partial\psi_z}{\partial n} \right], \quad (7)$$

where  $\mathbf{q}$  is the wavevector of the perturbation,  $\zeta$  the friction coefficient of the drag force between the polymer and the solvent,  $\psi_y$  and  $\psi_z$  normal stress coefficients related to the normal components  $\mathbf{P}_{yy}^v$  and  $\mathbf{P}_{zz}^v$  of the viscous pressure and  $\alpha = \partial \ln E / \partial \ln n$ , with  $E$  the elastic modulus. In the Rouse model,  $\alpha = 1$  and in the upper-convected Maxwell model both  $\psi_y$  and  $\psi_z$  vanish (see, for instance, Refs. [3,4]). Thus, in the situation studied in this paper, Eq. (7) reduce to  $D_{\text{eff}} = D$  and do not predict a shear-induced polymer separation (this is not so, of course, in the entangled polymer regime, to which Milner's paper is originally focused on). The reason of this discrepancy is a different definition for the nonequilibrium chemical potential, which in our case contributes to  $D_{\text{eff}}$  even in the dilute situation (see Refs. [4,12] for a thorough discussion), in agreement with experimental results reported in [22], and which are not described by Milner's choice of the chemical potential. Furthermore, our work has been focused on the radial component of the diffusion flow, because the other ones do not contribute, due to the symmetry of the situation, to the polymer separation. This is the reason we have not considered in full detail the directional dependence of a generalized diffusion coefficient, which is not necessary in the situation we are considering, but which could be of interest if we aimed to the analysis of light scattering in the flowing solution, which was the central of interest by Milner in Ref. [31].

Recall, finally, that in the literature one often refers to shear banding the appearance of bands with different shear rates but with almost uniform concentration [27–30]. This is found in fluids with elongated molecules exhibiting different orientations in the different bands. To describe this phenomenon, one uses a generalised constitutive equation for the viscous pressure, rather than for the diffusion flux. For instance, Dhont [27] has proposed for the viscous pressure a constitutive equation which for plane Couette flow reads

$$\mathbf{P}_{12}^v = -\eta\dot{\gamma} + \kappa \frac{\partial^2 \dot{\gamma}}{\partial y^2} \quad (8)$$

with  $\eta$  the viscosity and  $\kappa$  a new transport coefficient introduced ad hoc to take into account non-local effects in the viscous pressure. This is not incompatible with our model. Indeed, in EIT Eq. (2) used in this paper is compatible with a generalisation of the constitutive equation for  $\mathbf{P}^v$  in the form

$$\mathbf{P}^v = -2\eta(\nabla v)^s - 2\tau RT(\nabla J)^s, \quad (9)$$

where relaxation terms of the form  $\tau d\mathbf{P}^v/dt$  have been not

included for the sake of simplicity. Thus, in a homogeneous system, neglecting the first term in Eq. (3) and introducing the second term in Eq. (9) one obtains for plane Couette flow an equation analogous to Eq. (8). This points to the possibility that in actual situations both inhomogeneities in concentration and in shear rate may occur simultaneously, in such a way that both the point of view of the present paper and of Ref. [27] should be taken into account. Of course, there may also be situations in which one of both effects (diffusion or viscous pressure) is dominant in such a way that the other one may be neglected, thus leading to a considerable simplification as that considered here or, alternatively, that analysed in Ref. [27].

## Acknowledgements

We are pleased to dedicate this paper to Prof. Leopoldo S. García-Colín and Richard E. Nettleton on the occasion of their 70th anniversary. We acknowledge the financial support of the Dirección General de Investigación Científica y Técnica of the Spanish Ministry of Science and Technology under grant BFM2000-0351-003-0, of the Direcció General de Recerca of the Generalitat of the Catalonia under contract 1999-SGR00095 and of the Dirección General de Asuntos del Personal Académico of the UNAM (México) under grant IN-119200.

## References

- [1] Agarwal US, Dutta A, Mashelkar RA. Chem Engng Sci 1994;49:1693.
- [2] Onuki A. J Phys: Condens Matter 1997;9:6119.
- [3] Jou D, Casas-Vázquez J, Criado-Sancho M. Adv Polym Sci 1995;120:207.
- [4] Jou D, Casas-Vázquez J, Criado-Sancho M. Thermodynamics of fluids under flow. Berlin: Springer, 2000.
- [5] Jou D, Camacho J, Grmela M. Macromolecules 1991;24:3597.
- [6] Helfand E, Fredrickson H. Phys Rev Lett 1989;62:2468.
- [7] Clarke N, McLeish TCB. Phys Rev E 1998;57:R3731.
- [8] Ottinger HC. Colloid Polym Sci 1989;267:1.
- [9] Criado-Sancho M, Jou D, Casas-Vázquez J. Polymer 1995;36:4107.
- [10] Criado-Sancho M, Jou D, Casas-Vázquez J. Phys Rev E 1997;56:1887.
- [11] Jou D, Casas-Vázquez J, Criado-Sancho M. Physica A 1999;274:466.
- [12] Del Castillo LF, Criado-Sancho M, Jou D. Polymer 2000;41:2633.
- [13] Criado-Sancho M, Jou D, Casas-Vázquez J, del Castillo LF. Polymer 2000;41:8425.
- [14] Jou D, Casas-Vázquez J, Lebon G. Extended irreversible thermodynamics. 2nd ed. Berlin: Springer, 1996.
- [15] Jou D, Casas-Vázquez J, Lebon G. Rep Prog Phys 1988;51:1105.
- [16] Jou D, Casas-Vázquez J, Lebon G. Rep Prog Phys 1999;62:1035.
- [17] Nettleton RE, Sobolev SL. J Non-Equilib Thermodyn 1995;20:205.
- [18] Nettleton RE, Sobolev SL. J Non-Equilib Thermodyn 1996;21:297.
- [19] Maugin GA, Muschik W. J Non-Equilib Thermodyn 1994;19:217–50.
- [20] Verhas J. Thermodynamics and Rheology. Dordrecht: Kluwer Academic Publisher, 1997.
- [21] Goveas JL, Fredrickson GH. J Rheol 1999;43:1261.
- [22] MacDonald MJ, Muller SJ. J Rheol 1994;38:1235.
- [23] Dill KA, Zimm BH. Nucleic Acid Res 1979;7:735.

- [24] Dill KA. *Biophys Chem* 1979;10:327.
- [25] Shafer RH, Laiken N, Zimm BH. *Biophys Chem* 1974;2:180.
- [26] Nozières P, Quemada D. *Europhys Lett* 1986;2:129.
- [27] Dhont JKG. *Phys Rev E* 1999;60:4534.
- [28] McLeish TCB. *J Polym Sci, Part B: Polym Phys* 1987;25:2253.
- [29] Spanley NA, Yuan XF, Cates ME. *J Phys II* 1996;6:551.
- [30] Porte G, Barret J, Harden J. *J Phys II* 1997;7:459.
- [31] Milner ST. *Phys Rev E* 1993;48:3674.